

## Experimental High-Dimensional Quantum Teleportation

Xiao-Min Hu,<sup>1,2,\*</sup> Chao Zhang<sup>1,2,\*</sup>, Bi-Heng Liu<sup>1,2,†</sup>, Yu Cai,<sup>3</sup> Xiang-Jun Ye,<sup>1,2</sup> Yu Guo,<sup>1,2</sup> Wen-Bo Xing,<sup>1,2</sup>  
Cen-Xiao Huang,<sup>1,2</sup> Yun-Feng Huang,<sup>1,2</sup> Chuan-Feng Li,<sup>1,2,‡</sup> and Guang-Can Guo<sup>1,2</sup>

<sup>1</sup>CAS Key Laboratory of Quantum Information, University of Science and Technology of China,  
Hefei 230026, People's Republic of China

<sup>2</sup>CAS Center For Excellence in Quantum Information and Quantum Physics, University of Science and Technology of China,  
Hefei 230026, People's Republic of China

<sup>3</sup>Department of Applied Physics, University of Geneva, CH-1211 Geneva, Switzerland

ⓧ (Received 26 August 2019; revised 3 April 2020; accepted 6 November 2020; published 2 December 2020)

Quantum teleportation provides a way to transmit unknown quantum states from one location to another. In the quantum world, multilevel systems which enable high-dimensional systems are more prevalent. Therefore, to completely rebuild the quantum states of a single particle remotely, one needs to teleport multilevel (high-dimensional) states. Here, we demonstrate the teleportation of high-dimensional states in a three-dimensional six-photon system. We exploit the spatial mode of a single photon as the high-dimensional system, use two auxiliary entangled photons to realize a deterministic three-dimensional Bell state measurement. The fidelity of teleportation process matrix is  $F = 0.596 \pm 0.037$ . Through this process matrix, we can prove that our teleportation is both nonclassical and genuine three dimensional. Our work paves the way to rebuild complex quantum systems remotely and to construct complex quantum networks.

DOI: [10.1103/PhysRevLett.125.230501](https://doi.org/10.1103/PhysRevLett.125.230501)

Quantum teleportation [1,2] enables the rebuilding of arbitrary unknown quantum states without the transmission of a real particle. Previous efforts have shown the capability to rebuild qubit states and continuous variable states. Discrete variable states [3–9] and continuous variable states [10–13] in 1 degree of freedom have been transported. Recent work has also demonstrated the capability of teleporting multiple degrees of freedom of a single photon [14]. However, to teleport quantum states of a real particle, for example, a single photon, one needs to consider not only the two-level states (polarization), but also those multilevel states. For example, the orbital angular momentum [15,16], the temporal mode [17], the frequency mode [18], and the spatial mode [19–22] of a single photon are all natural attributes of multilevel states, which are exploited as high-dimensional systems. However, to teleport high-dimensional quantum states is still a challenge for two reasons. One is the generation of high-quality high-dimensional entanglement feasible for quantum teleportation. There has been much work on high-dimensional entanglement generation [15–22], including attempts to observe interference between different high-dimensional entangled pairs [23,24]. Nevertheless, the interference visibility between different pairs is still quite low at 63.5%. The other concerns performing a deterministic high-dimensional Bell state measurement (HDBSM). Here, we use the spatial mode (path) to encode the three-dimensional states that has been demonstrated to extremely high fidelity [20] and use an auxiliary entangled photon pair to perform the HDBSM. We thereby overcome these

obstacles and demonstrate the teleportation of a three-dimensional quantum state using the spatial mode of a single photon.

Suppose Alice wishes to teleport to Bob the quantum state of a single photon (photon 1, Fig. 1), encoded in the path mode as

$$|\varphi\rangle = \alpha|0\rangle + \beta|1\rangle + \gamma|2\rangle, \quad (1)$$

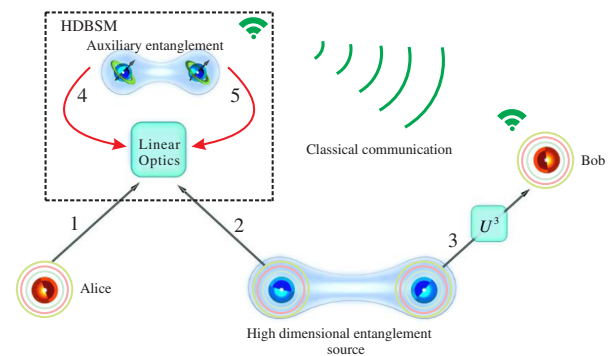


FIG. 1. Scheme for quantum teleportation of the high-dimensional states of a single photon. Alice wishes to teleport the high-dimensional quantum state of single photon 1 to Bob. Initially, Alice and Bob share a three-dimensional entangled photon pair 2–3. Then, Alice performs a high-dimensional Bell state measurement (HDBSM) assisted by another entangled photon pair 4–5 and sends the results to Bob through a classical channel. Finally, according to the results of HDBSM, Bob applies the appropriate three-dimensional Pauli operations on photon 3 to convert it into the original state of photon 1.

where  $|0\rangle$ ,  $|1\rangle$ , and  $|2\rangle$  denote the path degree of freedom (DOF). This DOF exists in an infinite dimensional space of the photonic system; here, we take only three dimensions as an example. The coefficients  $\alpha$ ,  $\beta$ , and  $\gamma$  are complex numbers satisfying  $|\alpha|^2 + |\beta|^2 + |\gamma|^2 = 1$ . Alice and Bob initially need to share a high-dimensional entangled photon pair (photons 2 and 3) in path

$$|\xi\rangle_{23} = (|00\rangle_{23} + |11\rangle_{23} + |22\rangle_{23})/\sqrt{3}. \quad (2)$$

Then, Alice performs a two-particle HDBSM on photons 1 and 2, which projects the two-photon state onto the basis of the nine orthogonal three-dimensional Bell states and discriminates one of them,

$$\begin{aligned} |\psi_{00}\rangle &= (|00\rangle + |11\rangle + |22\rangle)/\sqrt{3}, \\ |\psi_{10}\rangle &= (|00\rangle + e^{2\pi i/3}|11\rangle + e^{4\pi i/3}|22\rangle)/\sqrt{3}, \\ |\psi_{20}\rangle &= (|00\rangle + e^{4\pi i/3}|11\rangle + e^{2\pi i/3}|22\rangle)/\sqrt{3}, \\ |\psi_{01}\rangle &= (|01\rangle + |12\rangle + |20\rangle)/\sqrt{3}, \\ |\psi_{11}\rangle &= (|01\rangle + e^{2\pi i/3}|12\rangle + e^{4\pi i/3}|20\rangle)/\sqrt{3}, \\ |\psi_{21}\rangle &= (|01\rangle + e^{4\pi i/3}|12\rangle + e^{2\pi i/3}|20\rangle)/\sqrt{3}, \\ |\psi_{02}\rangle &= (|02\rangle + |10\rangle + |21\rangle)/\sqrt{3}, \\ |\psi_{12}\rangle &= (|02\rangle + e^{2\pi i/3}|10\rangle + e^{4\pi i/3}|21\rangle)/\sqrt{3}, \\ |\psi_{22}\rangle &= (|02\rangle + e^{4\pi i/3}|10\rangle + e^{2\pi i/3}|21\rangle)/\sqrt{3}. \end{aligned} \quad (3)$$

After the HDBSM, photons 1 and 2 are projected onto the state  $|\psi_{00}\rangle$  with a probability of  $1/9$ , then photon 3 is projected onto state  $|\varphi\rangle$ . For instances where photons 1 and 2 are projected onto the other eight three-dimensional Bell states, Bob needs to perform a three-dimensional unitary operation on photon 3 to rotate the state of photon 3 to  $|\varphi\rangle$  according to the measurement results of photons 1 and 2.

However, HDBSM is still a challenge with linear optics [25,26]. Although one can classify high-dimensional entangled states into several categories [27,28], one cannot identify any of them. The possible solution to this HDBSM is to introduce an auxiliary system. Here, we introduce a pair of assistant entangled photons to complete the HDBSM.

The Bell state measurement (BSM) of a two-dimensional polarized state is divided into two steps [29]. The four Bell states are first divided into two categories ( $(|HH\rangle \pm |VV\rangle)/\sqrt{2}$  and  $(|HV\rangle \pm |VH\rangle)/\sqrt{2}$ ) by a polarizing beam splitter (PBS) according to classical terms. Second, the two states are distinguished with different phases by projecting onto basis  $|H \pm V\rangle/\sqrt{2}$ . The structure of HDBSM in our system is similar to that of qubit polarized BSM. According to classical terms, nine three-dimensional Bell states are divided into three categories, then, the localized projection measurement is used to identify the three-dimensional Bell states.

Figure 2 illustrates our linear optical scheme for teleporting the three-dimensional quantum states. The first step is to divide nine Bell states into three categories according to classical terms  $|i, i\rangle$ ,  $|i, i+1\rangle$ , and  $|i, i+2\rangle$ ,  $i \in \{0, 1, 2\}$  under modulo-3 arithmetic. Photons 1 and 2 are sent to a PBS, which transmits horizontally polarized terms ( $|H\rangle$ ) and reflects vertically polarized terms ( $|V\rangle$ ). In the three-dimensional path state, we control the polarization of each path to satisfy ( $|0\rangle \rightarrow |H\rangle$ ,  $|1\rangle \rightarrow |V\rangle$ , and  $|2\rangle \rightarrow |H\rangle$ ). After the PBS, we postselect the event in which there is one and only one photon in each outport. For the nine classical terms of the three-dimensional Bell states ( $|i, j\rangle$ ,  $i, j \in \{0, 1, 2\}$ ), five of them are selected ( $|i, j\rangle$  with  $i+j$  even).

The second step is to use a local projection measurement to determine which Bell state is postselected through  $|\psi_{00}\rangle$ ,  $|\psi_{10}\rangle$  and  $|\psi_{20}\rangle$  (here, terms  $|20\rangle$  and  $|02\rangle$  are noise terms and are cancelled later). We can construct an arbitrary single qutrit basis (e.g.,  $(|0\rangle + |1\rangle + |2\rangle)/\sqrt{3}$ ) by half-wave plates (HWPs), beam displacers (BDs) and PBSs, so that we can determine whether the measured state is  $|\psi_{00}\rangle$  by measuring this basis on both sides [20].

To cancel the disturbance terms ( $|20\rangle$  and  $|02\rangle$ ), we introduce another entangled photon pair [30]. Hence, we can distinguish at least one Bell state deterministically. For Bell states  $|\psi_{10}\rangle$  and  $|\psi_{20}\rangle$ , we need to select different local projection measurements. Finally, we have teleported a three-dimensional quantum state with a success probability of  $1/54$ . To increase the success probability, we use the nonmaximally entangled state  $(2|00\rangle + 2|11\rangle + |22\rangle)/3$  to replace the maximally entangled state  $|\xi\rangle_{23}$ , and adjust the measurement base on HDBSM correspondingly, this increases the success probability of teleportation to  $1/18$  while does not affect the fidelity [30]. This method of completing HDBSM in linear optical systems can be extended to higher dimensions and can be applied to different degrees of freedom such as orbital angular momentum (OAM). For  $d$ -dimensional systems, we only need  $\lceil \log_2(d) \rceil - 1$  pairs of auxiliary entangled photons [30].

The implementation of the HDBSM requires Hong-Ou-Mandel (HOM)-type interference between indistinguishable single photons with good temporal, spatial, and spectral overlap. We use a narrow band interference filter (3 nm) and a single-mode fiber to improve the visibility of HOM interference. For photon 3 and photon  $t$ , we use a broadband interference filter (8 nm) to increase the coincidence efficiency.

The verification of the teleportation results relies on the coincidence events of six photons. To suppress the statistical error, the data collection time is tens of hours. Hence, the stability of the whole system becomes a crucial aspect for the experiment. In our system, the HOM interference between the different photons is stable enough [34,35], whereas the interference between different spatial modes after passing through the single-mode fibers is not.

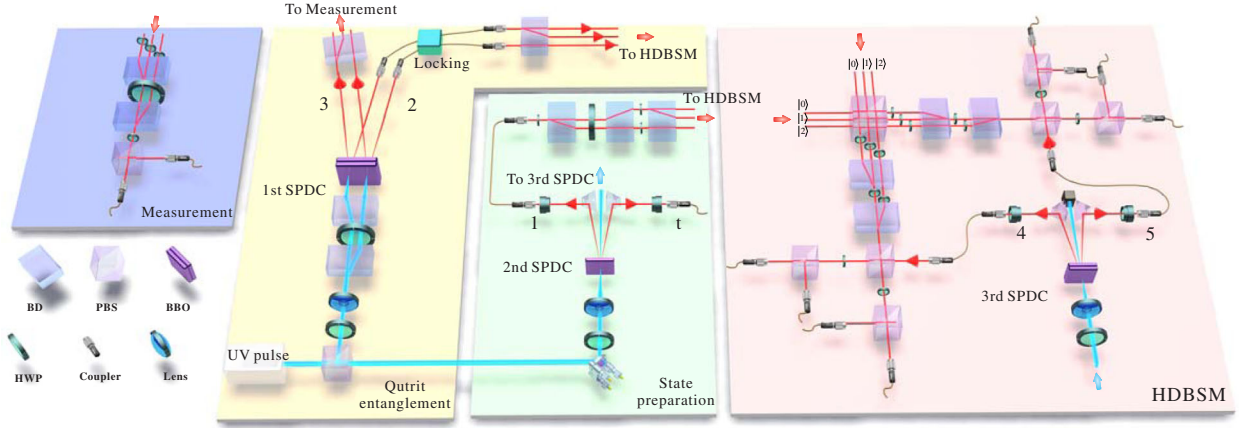


FIG. 2. Experimental setup for teleporting a qutrit state of a single photon. A pulsed ultraviolet (UV) laser is focused on three sets of  $\beta$ -barium borate (BBO) crystals and produces three photon pairs in 2–3, 1– $t$ , and 4–5. The first pair, 2–3, is qutrit-qutrit entanglement in path DOF shared by Alice and Bob. The second pair, 1– $t$ , photon 1 is initialized in various states ( $|\varphi_1\rangle - |\varphi_{10}\rangle$ ) to be teleported, triggered by its twisted photon  $t$ . The third pair, 4–5, is a polarization-entangled state, used as an ancillary pair for performing a HDBSM on photons 1 and 2.

Here, we use a fiber phase locking system [30] to maintain a phase-stable interferometer. The measured interference visibility remained above 0.98 in 45 h [30].

We prepared ten different initial states to be teleported:  $|\varphi_1\rangle = |0\rangle$ ,  $|\varphi_2\rangle = |1\rangle$ ,  $|\varphi_3\rangle = |2\rangle$ ,  $|\varphi_4\rangle = (|0\rangle + |1\rangle)/\sqrt{2}$ ,  $|\varphi_5\rangle = (|0\rangle + i|1\rangle)/\sqrt{2}$ ,  $|\varphi_6\rangle = (|0\rangle + |2\rangle)/\sqrt{2}$ ,  $|\varphi_7\rangle = (|0\rangle + i|2\rangle)/\sqrt{2}$ ,  $|\varphi_8\rangle = (|1\rangle + |2\rangle)/\sqrt{2}$ ,  $|\varphi_9\rangle = (|1\rangle + i|2\rangle)/\sqrt{2}$ , and  $|\varphi_{10}\rangle = (|0\rangle + |1\rangle + |2\rangle)/\sqrt{3}$ . The first nine states ( $|\varphi_1\rangle - |\varphi_9\rangle$ ) constitute a complete orthogonal basis in three-dimensional space; the last state  $|\varphi_{10}\rangle$  is a linear-dependent superposition of quantum states in this space. All these states are prepared by the BDs, QWPs, and HWPs.

To evaluate the performance of the high-dimensional teleportation, we reconstruct the density matrix of  $|\varphi_1\rangle - |\varphi_{10}\rangle$  by state tomography. Conditioned on the detection of the trigger photon and the four-photon coincidence after the HDBSM, we registered the photon counts of teleported photon 1. As shown in Fig. 3, the average fidelity of states  $|\varphi_1\rangle - |\varphi_{10}\rangle$  is  $F = 0.685 \pm 0.027$ , which is significantly higher than that of qutrit nonclassical teleportation bound ( $>0.5$  [36,37]).

All reported data are the raw data without background subtraction. The main sources of error include double pair emission, imperfect initial states, entanglement of photons 2–3 and 4–5, two-photon interference, and phase stabilization. We note that the teleportation fidelities of the states are affected differently by errors from the various sources. The fidelity of  $|\varphi_1\rangle - |\varphi_3\rangle$  is higher than that of  $|\varphi_4\rangle - |\varphi_{10}\rangle$ . The reason is that imperfect interference does not affect the first three quantum states, but the latter.

The first nine states ( $|\varphi_1\rangle - |\varphi_9\rangle$ ) are a set complete basis for three-dimensional tomography. The reconstructed density matrices of the teleported quantum states allow us to fully characterize the teleportation procedure by

quantum process tomography [39]. We can completely describe the effect of teleportation on the input states  $\rho_{\text{ideal}}$  by determining the process matrix  $\chi$ , defined by  $\rho = \sum_{l,k=0}^8 \chi_{lk} \sigma_l \rho_{\text{ideal}} \sigma_k$ , where  $\sigma_0 - \sigma_8$  are the Pauli matrices for three dimension [38]. The ideal process matrix of quantum teleportation  $\chi_{\text{ideal}}$  has only one nonzero component ( $\chi_{\text{ideal}})_{00} = 1$ , represents that the process of

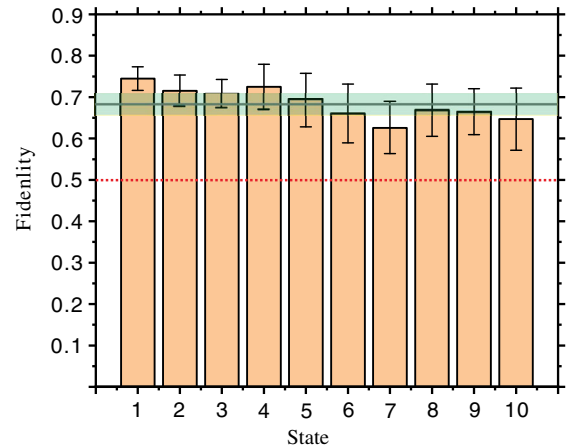


FIG. 3. Experimental results for quantum teleportation of three-dimensional single photon states  $|\varphi_1\rangle - |\varphi_{10}\rangle$ . We reconstruct the density matrix of the three-dimensional states by state tomography [38], and then obtain the fidelity of each state. Density matrix of the qutrits is reconstructed from a set of 9 measurements represented by operators  $u_i$  (with  $i = 1, 2, \dots, 9$ ) and  $u_i = |\Psi_i\rangle\langle\Psi_i|$ . Kets  $|\Psi_i\rangle$  are selected from the following setting  $|0\rangle, |1\rangle, |2\rangle, (|0\rangle + |1\rangle)/\sqrt{2}, (|0\rangle + i|1\rangle)/\sqrt{2}, (|0\rangle + |2\rangle)/\sqrt{2}, (|0\rangle + i|2\rangle)/\sqrt{2}, (|1\rangle + |2\rangle)/\sqrt{2}, (|1\rangle + i|2\rangle)/\sqrt{2}$ . Average fidelity ( $F = 0.685 \pm 0.027$ ) of 10 states is significantly higher than that of nonclassical quantum teleportation bound (0.5). Error bars are calculated from Poissonian counting statistics of the raw detection events.



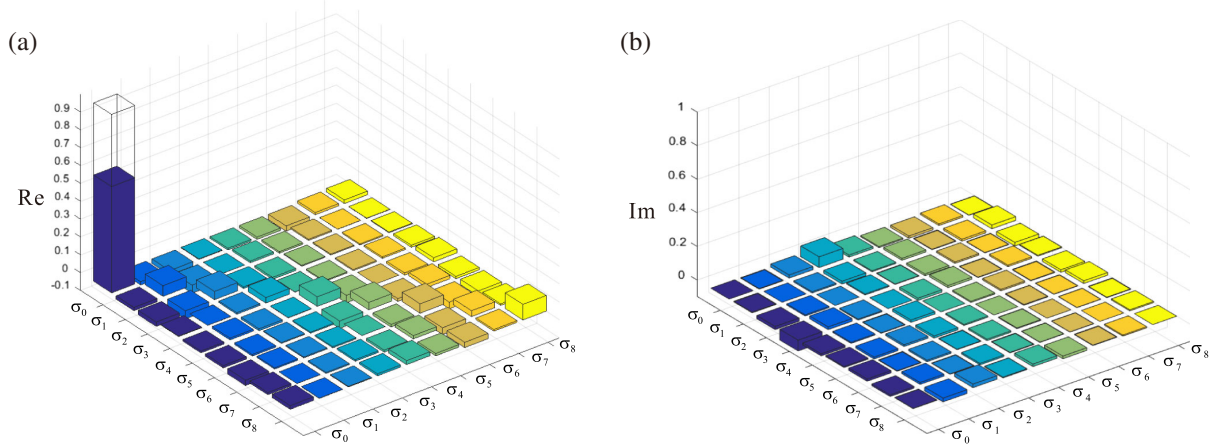


FIG. 4. Quantum process tomography of three-dimensional quantum teleportation. (a),(b), The real  $[\text{Re}(\chi_{lk})]$  and imaginary  $[\text{Im}(\chi_{lk})]$  values of the components of the reconstructed quantum process matrix, with  $l, k = 0, 1, 2, \dots, 8$ . The results of the state tomography of the nine teleported states,  $|\varphi_1\rangle - |\varphi_9\rangle$ , are employed to reconstruct the process matrix of teleportation. The operator  $\sigma_0 - \sigma_8$  are Pauli matrices in three dimensions. For the ideal case, the only nonzero component of the process matrix of quantum teleportation,  $\chi_{\text{ideal}}$ , is  $(\chi_{\text{ideal}})_{00} = 1$ , which is indicated by the transparent column.

teleportation is perfect. Figure 4 shows the real and imaginary components of  $\chi$  for quantum teleportation based on our experimental results, respectively. The process fidelity of our experiment was  $f_{\text{process}} = \text{Tr}(\chi_{\text{ideal}}\chi) = 0.596 \pm 0.037$ .

In general, to demonstrate that the three-dimensional teleportation is nonclassical using average fidelity, one need to measure 12 states from four mutually unbiased bases settings ( $|\psi_1\rangle - |\psi_{12}\rangle$ ) [30,40]. In the three-dimensional case, the lower bound of average fidelity for nonclassical teleportation is 0.5. This condition can be converted to process fidelity [41] and the lower bound of process fidelity is  $1/3$ . In our experiment, the measured process fidelity is  $f_{\text{process}} = 0.596 \pm 0.037$ , which is 7 standard deviations above the fidelity of  $1/3$ , and proves that our teleportation is nonclassical.

For high-dimensional teleportation, it is not enough to only prove that teleportation is nonclassical. Genuine  $d$ -dimensional teleportation should be distinguished from the low dimensional case, excluding the hypothesis that the teleportation can be expressed in a smaller dimension. In our case, we need to exclude qubit and make sure that we have completed the genuine three-dimensional teleportation. In Ref. [42], two-dimensional states are transmitted, it is found that the maximum fidelity with state  $(|0\rangle + |1\rangle + |2\rangle)/\sqrt{3}$  is  $2/3$ . Therefore, quantum states with fidelity more than  $2/3$  are genuine three-dimensional states. However, this is a sufficient but not a necessary condition. For some states (like  $\sqrt{1/8}|0\rangle + \sqrt{1/8}|1\rangle - \sqrt{3/4}|2\rangle$ ), the fidelity cannot reach  $2/3$ , but they are still genuine three-dimensional coherent superposition states. If someone who can transmit all qubit states is unable to simulate a teleportation, then it is reasonable to say that the teleportation performed is genuine three dimensional. We assume

that the qubit state  $[\rho_{\text{qubit}} = (P_1\rho_{01} + P_2\rho_{02} + P_3\rho_{12})]$  is incoherent at different subspaces ( $\{|0\rangle, |1\rangle\}$ ,  $\{|0\rangle, |2\rangle\}$ ,  $\{|1\rangle, |2\rangle\}$ ). If we cannot use this qubit state to simulate the state after teleportation, then we prove that our teleportation state is in the state of three levels of coherent superposition. First, we derive a nonlinear criterion [30], which is more powerful than the fidelity criterion. This criterion can be used to determine states like  $\sqrt{1/8}|0\rangle + \sqrt{1/8}|1\rangle - \sqrt{3/4}|2\rangle$  are genuine three-dimensional states. Of course, this criterion is still not a necessary and sufficient condition. We define the robustness ( $\mu$ ) [43] of the genuine three-dimensional state. The optimal solution  $\mu^*$  of this problem gives the minimum amount of “white noise” that has to be added to the qutrit state such that the mixture can be simulated by qubit states [30]. If  $\mu > 0$ , we can certify that this state is a genuine three-dimensional state. On the contrary, if  $\mu = 0$ , the state is not a genuine three-dimensional state. We choose 400 maximum coherent superposition states  $[1/\sqrt{3}(|0\rangle + e^{i\varphi_1}|1\rangle + e^{i\varphi_2}|2\rangle)]$ , where  $\varphi_1, \varphi_2$  are 20 phases at equal interval in  $[0, \pi]$  as the input states, and then through the evolution of  $\chi$  matrix. After the semidefinite program, we find that 149 states can be simulated by qubit, while 251 states cannot be simulated. The average  $\mu$  of these states that can not be simulated is  $\mu = 0.111 \pm 0.034 > 0$ . This means that within three standard deviation ranges, using qubit states cannot simulate our teleportation process. This result can prove that our teleportation is beyond qubit. All the errors are obtained by raw data through the Monte Carlo method, in which all the generated data have the same Poissonian error as the raw data.

In summary, we have reported the quantum teleportation of high-dimensional quantum states of a single quantum particle, demonstrating the capability to control coherently

and teleport simultaneously a high-dimensional state of a single object. The generation of a high-quality high-dimensional multiphoton state will stimulate the research on high-dimensional quantum information tasks, and entanglement-assisted methods for HDBSM are feasible for other high-dimensional quantum information tasks.

We thank Che-Ming Li for valuable information. This work was supported by the National Key Research and Development Program of China (No. 2017YFA0304100, No. 2016YFA0301300, and No. 2016YFA0301700), NSFC (No. 11774335, No. 11734015, No. 11874345, No. 11821404, No. 11805196, and No. 11904357), the Key Research Program of Frontier Sciences, CAS (No. QYZDY-SSW-SLH003), Science Foundation of the CAS (ZDRW-XH-2019-1), the Fundamental Research Funds for the Central Universities, Science and Technological Fund of Anhui Province for Outstanding Youth (2008085J02), Anhui Initiative in Quantum Information Technologies (No. AHY020100, No. AHY060300) and Swiss National Science Foundation (Starting Grant DIAQ, NCCR-QSIT).

\*These authors contributed equally to this work.

<sup>†</sup>bhliu@ustc.edu.cn

<sup>‡</sup>cfl@ustc.edu.cn

- [1] C. H. Bennett, G. Brassard, C. Crépeau, R. Jozsa, A. Peres, and W. K. Wootters, Teleporting an Unknown Quantum State via Dual Classic and Einstein-Podolsky-Rosen Channels, *Phys. Rev. Lett.* **70**, 1895 (1993).
- [2] S. Pirandola, J. Eisert, C. Weedbrook, A. Furusawa, and S. L. Braunstein, Advances in quantum teleportation, *Nat. Photonics* **9**, 641 (2015).
- [3] D. Bouwmeester, J.-W. Pan, K. Mattle, M. Eibl, H. Weinfurter, and A. Zeilinger, Experimental quantum teleportation, *Nature (London)* **390**, 575 (1997).
- [4] M. A. Nielsen, E. Knill, and R. Laflamme, Complete quantum teleportation using nuclear magnetic resonance, *Nature (London)* **396**, 52 (1998).
- [5] D. Fattal, E. Diamanti, K. Inoue, and Y. Yamamoto, Quantum Teleportation with a Quantum Dot Single Photon Source, *Phys. Rev. Lett.* **92**, 037904 (2004).
- [6] M. D. Barrett, J. Chiaverini, T. Schaetz, J. Britton, W. M. Itano, J. D. Jost, E. Knill, C. Langer, D. Leibfried, R. Ozeri, and D. J. Wineland, Deterministic quantum teleportation of atomic qubits, *Nature (London)* **429**, 737 (2004).
- [7] M. Riebe, H. Häffner, C. F. Roos, W. Hänsel, J. Benhelm, G. P. T. Lancaster, T. W. Körber, C. Becher, F. Schmidt-Kaler, D. F. V. James, and R. Blatt, Deterministic quantum teleportation with atoms, *Nature (London)* **429**, 734 (2004).
- [8] J. F. Sherson, H. Krauter, R. K. Olsson, B. Julsgaard, K. Hammerer, I. Cirac, and E. S. Polzik, Quantum teleportation between light and matter, *Nature (London)* **443**, 557 (2006).
- [9] S. Olmschenk, D. N. Matsukevich, P. Maunz, D. Hayes, L.-M. Duan, and C. Monroe, Quantum teleportation between distant matter qubits, *Science* **323**, 486 (2009).
- [10] A. Furusawa, J. L. Sørensen, S. L. Braunstein, C. A. Fuchs, H. J. Kimble, and E. S. Polzik, Unconditional quantum teleportation, *Science* **282**, 706 (1998).
- [11] N. Takei, H. Yonezawa, T. Aoki, and A. Furusawa, High-Fidelity Teleportation beyond the No-Cloning Limit and Entanglement Swapping for Continuous Variables, *Phys. Rev. Lett.* **94**, 220502 (2005).
- [12] H. Yonezawa, S. L. Braunstein, and A. Furusawa, Experimental Demonstration of Quantum Teleportation of Broadband Squeezing, *Phys. Rev. Lett.* **99**, 110503 (2007).
- [13] N. Lee, H. Benichi, Y. Takeno, S. Takeda, J. Webb, E. Huntington, and A. Furusawa Teleportation of nonclassical wave packets of light, *Science* **332**, 330 (2011).
- [14] X.-L. Wang, X.-D. Cai, Z.-E. Su, M.-C. Chen, D. Wu, L. Li, N.-L. Liu, C.-Y. Lu, and J.-W. Pan, Quantum teleportation of multiple degrees of freedom in a single photon, *Nature (London)* **518**, 516 (2015).
- [15] A. C. Dada, J. Leach, G. S. Buller, M. J. Padgett, and E. Andersson, Experimental high-dimensional two-photon entanglement and violations of generalized Bell inequalities, *Nat. Phys.* **7**, 677 (2011).
- [16] M. Krenn, M. Huber, R. Fickler, R. Lapkiewicz, S. Ramelow, and A. Zeilinger, Generation and confirmation of a  $(100 \times 100)$ -dimensional entangled quantum system, *Proc. Natl. Acad. Sci. U.S.A.* **111**, 6243 (2014).
- [17] M. Martin, T. Guerreiro, A. Tiranov, S. Designolle, F. Fröwis, N. Brunner, M. Huber, and N. Gisin, Quantifying Photonic High-Dimensional Entanglement, *Phys. Rev. Lett.* **118**, 110501 (2017).
- [18] M. Kues, C. Reimer, P. Roztocky, L. R. Cortés, S. Sciara, B. Wetzl, Y. Zhang, A. Cino, S. T. Chu, B. E. Little *et al.*, On-chip generation of high-dimensional entangled quantum states and their coherent control, *Nature (London)* **546**, 622 (2017).
- [19] C. Schaeff, R. Polster, M. Huber, S. Ramelow, and A. Zeilinger, Experimental access to high-dimensional entangled quantum systems using integrated optics. *Optica* **2**, 523 (2015).
- [20] X.-M. Hu, J.-S. Chen, B.-H. Liu, Y. Guo, Y.-F. Huang, Z.-Q. Zhou, Y.-J. Han, C.-F. Li, and G.-C. Guo, Experimental Test of Compatibility-Loophole-Free Contextuality with Spatially Separated Entangled Qutrits, *Phys. Rev. Lett.* **117**, 170403 (2016).
- [21] X.-M. Hu, W.-B. Xing, B.-H. Liu, Y.-F. Huang, C.-F. Li, G.-C. Guo, P. Erker, and M. Huber, Efficient Generation of High-Dimensional Entanglement Through Multipath Down-Conversion, *Phys. Rev. Lett.* **125**, 090503 (2020).
- [22] N. H. Valencia, V. Srivastav, M. Pivoluska, M. Huber, N. Friis, W. McCutcheon, and M. Malik, High-dimensional pixel entanglement: Efficient generation and certification. [arXiv:2004.04994](https://arxiv.org/abs/2004.04994).
- [23] M. Erhard, M. Malik, M. Krenn, and A. Zeilinger, Experimental Greenberger-Horne-Zeilinger entanglement beyond qubits, *Nat. Photonics* **12**, 759 (2018).
- [24] M. Malik, M. Erhard, M. Huber, M. Krenn, R. Fickler, and A. Zeilinger, Multi-photon entanglement in high dimensions, *Nat. Photonics* **10**, 248 (2016).
- [25] J. Calsamiglia, Generalized measurements by linear elements, *Phys. Rev. A* **65**, 030301(R) (2002).

- [26] H. Zhang, C. Zhang, X.-M. Hu, B.-H. Liu, Y.-F. Huang, C.-F. Li, and G.-C. Guo, Arbitrary two-particle high-dimensional Bell-state measurement by auxiliary entanglement, *Phys. Rev. A* **99**, 052301 (2019).
- [27] X.-M. Hu, Y. Guo, B.-H. Liu, Y.-F. Huang, C.-F. Li, and G.-C. Guo, Beating the channel capacity limit for superdense coding with entangled ququarts, *Sci. Adv.* **4**, eaat9304 (2018).
- [28] A. D. Hill, T. M. Graham, and P. G. Kwiat, *Hyperdense Coding with Single Photons* (Optical Society of America, Washington, DC, 2016), <https://doi.org/10.1364/FIO.2016.FW2B.2>.
- [29] B.-H. Liu, X.-M. Hu, Y.-F. Huang, C.-F. Li, G.-C. Guo, A. Karlsson, E.-M. Laine, S. Maniscalco, C. Macchiavello, and J. Piilo, Efficient superdense coding in the presence of non-Markovian noise, *Europhys. Lett.* **114**, 10005 (2016).
- [30] See Supplemental Material at <http://link.aps.org/supplemental/10.1103/PhysRevLett.125.230501> for details, which includes Ref. [31–33].
- [31] X.-M. Hu, B.-H. Liu, Y. Guo, G.-Y. Xiang, Y.-F. Huang, C.-F. Li, G.-C. Guo, M. Kleinmann, T. Vértesi, and A. Cabello, Observation of Stronger-Than-Binary Correlations with Entangled Photonic Qutrits, *Phys. Rev. Lett.* **120**, 180402 (2018).
- [32] A. Gilchrist, N. K. Langford, and M. A. Nielsen, Distance measures to compare real and ideal quantum processes, *Phys. Rev. A* **71**, 062310 (2005).
- [33] R. B. A. Adamson and A. M. Steinberg, Improving Quantum State Estimation with Mutually Unbiased Bases, *Phys. Rev. Lett.* **105**, 030406 (2010).
- [34] C. Zhang, Y.-F. Huang, Z. Wang, B.-H. Liu, C.-F. Li, and G.-C. Guo, Experimental Greenberger-Horne-Zeilinger-Type Six-Photon Quantum Nonlocality, *Phys. Rev. Lett.* **115**, 260402 (2015).
- [35] X.-M. Hu, C. Zhang, C.-J. Zhang, B.-H. Liu, Y.-F. Huang, Y.-J. Han, C.-F. Li, and G.-C. Guo, Experimental certification for nonclassical teleportation, *Quantum Eng.* **1**, e13 (2019).
- [36] A. Hayashi, T. Hashimoto, and M. Horibe, Reexamination of optimal quantum state estimation of pure states, *Phys. Rev. A* **72**, 032325 (2005).
- [37] D. Brub and C. Macchiavello, Optimal state estimation for d-dimensional quantum systems, *Phys. Lett. A* **253**, 249 (1999).
- [38] R. T. Thew, K. Nemoto, A. G. White, and W. J. Munro, Qudit quantum-state tomography, *Phys. Rev. A* **66**, 012303 (2002).
- [39] J. Fiurášek and Z. Hradil, Maximum-likelihood estimation of quantum processes, *Phys. Rev. A* **63**, 020101(R) (2001).
- [40] I. D. Ivanovic, Geometrical description of quantum state determination, *J. Phys. A* **14**, 3241 (1981).
- [41] A. Gilchrist, N. K. Langford, and M. A. Nielsen, Distance measures to compare real and ideal quantum processes, *Phys. Rev. A* **71**, 062310 (2005).
- [42] Y.-H. Luo, H.-S. Zhong, M. Erhard, X.-L. Wang, L.-C. Peng, M. Krenn, X. Jiang, L. Li, N.-L. Liu, C.-Y. Lu, A. Zeilinger, and J. W. Pan, Quantum Teleportation in High Dimensions, *Phys. Rev. Lett.* **123**, 070505 (2019).
- [43] D. Cavalcanti, P. Skrzypczyk, and I. Šupić, All Entangled States can Demonstrate Nonclassical Teleportation, *Phys. Rev. Lett.* **119**, 110501 (2017).